White Paper VIII

What Is Information Entanglement and Why Is It So Important to Psychoenergetic Science?

by

William A. Tiller, Ph.D. and Walter E. Dibble, Jr., Ph.D.

The William A. Tiller Foundation

<u>Background</u>

Psychoenergetic science[1] can metaphorically be described by the reaction equation

$$\text{Mass} \Leftrightarrow \text{Energy} \Leftrightarrow \text{Information} \Leftrightarrow \text{Consciousness,} \quad (1)$$

and is a major expansion of today's orthodox science to include consciousness as a significant experimental variable in the study of nature's manifold expressions. Here, information is the bridging element that connects consciousness to the thermodynamic structure of orthodox science (the uncoupled state of physical reality[2]). Although we don't presently have an agreed-upon definition of consciousness, we can agree that it manipulates information in all its various forms. Further, we experimentally and theoretically[3] agree that any process in nature that generates an increase in information, ΔI, automatically generates a decrease in thermodynamic entropy, ΔS, given by

$$\Delta I = -\Delta S = -k_B \ln(P_0/P_1). \qquad (2)$$

Here, **k_B** = Boltzmann's constant = 1.38×10^{-16} ergs per degree centigrade and **P** is the number of microscopic elementary complexions (distinguishable states) in the system[3], where the subscripts 0 and 1 refer to the initial and final states of the system, respectively.

This important contribution to the thermodynamic free energy, G, of the system actually restores thermodynamic potential to our universe, where

$$G = PV + E - T\left(S_0 - \sum_j \Delta I_j\right). \qquad (3)$$

Here, P = pressure, V = volume, E = energy and T = temperature. S_0 is the normal entropy of the system (which generally is positive and increases with most processes in nature) and the subscript j refers to the various levels of reality being taken into account. For the uncoupled state, $\sum_j \Delta I_j$ is given by equation 2; whereas, for the coupled state of physical reality[2], both the electromagnetic energy contribution ($k=k_B$) <u>and</u> the magnetoelectric energy contribution ($k=k_m$) must be taken into account. Our present working hypothesis is that $k_m \sim 10^{10} k_B$ so that this contribution to Equation 3 becomes more

and more dominating as a thermodynamic driving force in nature as one investigates higher and higher dimensional realities.

In Equation 1 of White Paper I[2], the properties of materials for the partially coupled state of physical reality are considered and, for this level of reality[4], macroscopic, room temperature, large size spaces have exhibited information entanglement over both small D-space distances (~ 100 yards), intermediate distances (~ 20 miles) and large distances(~ 6000 miles)[5,1]. By this, we mean that pH-measurements in laboratory A, which contains an active intention-host device directed to a specific pH change is reasonably well replicated in laboratory B, far distant from laboratory A, which has never contained such an intention-host device. In this White Paper, compelling experimental evidence will be visited and discussed in an attempt to understand this odd behavior (by orthodox physics standards). We will begin by first mentioning quantum entanglement and some of its limitations.

Quantum Entanglement

In quantum information science, groups of two or more quantum objects can have energetic states that are **entangled**. These states can have properties unlike anything in classical physics. In classical information science, a familiar example is a string of bits, encoded via real physical objects, like the spin of an atomic nucleus or the polarization of a photon of light, but abstractly by **zeros** (down-state) or **ones** (up-state). A qubit, the quantum version of a bit, has many more possible states than just these two. The quantum version reveals that **each** of these two states is split into a multiplicity of states so that the final outcome can be weighted in many, many different ways.[6]

Entanglement, as explained by Aczel[7] is an application of the superposition principle to a **system** comprised of two or more subsystems. In his case, he lets each of the subsystems be a single particle and asks "What does it mean to say that the two particles are entangled?" He postulates that Particle 1 has equal probability of being in states A or C, which represent different physical locations. Particle 2, on the other hand, has equal probability of being in states B or D which have two additional, different locations. When the overall system of these two particles has fully reacted with each other and is in **the product state**, AB, Particle 1 is known to be in State A while Particle 2 is known to be in State B. Similarly, the other possible product state CD has Particles 1 and 2 in States C and D, respectively. The implicit assumption, here, is that non-local states are connected somehow.

Since the mathematical aspects of the superposition principle **also** allows the system to be in a combination of product states, the state AB + CD is also an allowed state and thus, for the entire system, this is called an **entangled state**. This entangled state says that there are now Particle 1 and 2 possibilities that are strongly **correlated**. Thus, if an experimental measurement finds Particle 1 in State **A**, then Particle 2 "must" be in State **B** and cannot be in State C or D. This means that, when Particles 1 and 2 are entangled, there is no way to characterize either one of them by itself, as if it were isolated from the other. In the **superposition state** the two are strongly linked and **do not** have independence of action!

Erwin Schröedinger, Nobel Prize Winner in the 1930's for his mathematical formulation of **the probability wave function equation** for quantum mechanics, was the very first to predict the existence of quantum entanglement for fundamental particles and photons. Einstein labeled this "spooky action at a distance".

In 2003, Ghosh[8] and his collaborators at the University of Chicago analyzed ten year old experimental data on some very low temperature (~1° Kelvin) magnetic susceptibility and heat capacity of a small magnetic salt crystal containing holmium atoms and compared them to quantum theory. Above ~1°K, classical mechanics theory gave a good match to the experimental data. However, quantum mechanical entanglement contributions had to be added in order to give a good match with his experimental data below 1°K.

This is typical of many, many experiments carried out to distinguish classical vs. quantum type of behavior as a function of system temperature and system size. It has been generally found that (1) as the temperature increases from very low values, a few degrees, and (2) the system size increases from ~two photons or fundamental particles to a very small crystal, the boundary between quantum-like behavior and classical-like behavior becomes very fuzzy. Well-developed classical-like behavior sets in far below room temperature and system sizes well below 1 cubic centimeter.

The effect validated by Ghosh et al[8] was first predicted by Vedral[9] two years earlier. If the theoretical idea of Reznik[10] is true, that all of empty space (the physical vacuum) is filled with entangled particles, then quantum-like behavior might be retained up to almost room temperature. Continuing along this line of thought, Brukner, Vedral and others[11] showed theoretically that time can become entangled too. This latter information puts space and time on an equal footing in quantum mechanics which is an absolute "no-no" for our "present-day" formulation of quantum mechanics.

Partially Coupled State Space Entanglements

In White Papers I and III[1,11], a measured material property is given approximately by

$$Q_M(t) \approx Q_e + \alpha_{eff}(t)Q_m(t) \qquad (4)$$

where $\alpha_{eff}(t)$ is the time-dependent coupling coefficient between the electric charge, atom/molecule world, where Q_e is its material property value, and the magnetic charge, information wave world, where Q_m is its material property value.

Mathematically Q_e and Q_m generally possess very different kinds of qualities. Most often Q_e is a scalar (only one number is needed to define a property at one point in space); however, the pieces of the puzzle that ultimately leads to Q_m are vectors (one needs three numbers to define a property at one point in space). To illustrate the complex issues involved, we must first recognize that we are dealing, here, with the magnetic information wave domain whose different material properties are all, at least, of a vectorial character. Further, an experimental measurement system is comprised of a number of subsystem R-space vectors that must be appropriately added to one another in a head to tail arrangement to form the total R-space system one is trying to measure.

As a very simple example, suppose we consider two pH-measuring systems probing the same experimental space (a room in a building for example). For either of these devices, measurement involves sampling the space at a particular location in the room. The whole system involves (1) the room and its history, (2) the room's air temperature, (3) the character of the air in the room, (4) the pH-electrode and (5) subtle and not visible factors if the room is in the uncoupled state. However, we are going to greatly simplify things in order to make a pedagogical point. We are dealing, here, with a partially coupled state (α_{eff} is non-zero) and will consider only two factors to be dominant and all the others can be neglected. These two factors are (1) the pH-electrode change and (2) the space change relative to the uncoupled state reality. Thus, since we have found a procedure for converting pH(t)-data in a space to excess thermodynamic free energy for the H^+-ion, $\delta G^*_{H+}(t)$, in that space[11], the actual measured value of (M) can be approximated by

$$\boxed{\delta G^*_{H+}(M) \approx \delta G^*_{H+}(E) + \delta G^*_{H+}(S^*).}$$

For simplicity, each of the R-space terms on the right is a vector and must be vectorially added to obtain the appropriate system vector for one measurement device. Since we are using two measurement systems, we must add each of the device system vectors to obtain the total system vector. Let us first see how this is done from a geometrical perspective to help us understand what we are dealing with. Then, we can more readily convert this vector algebra and, finally, we can take the last few steps needed to obtain Q_m.

      This is an extremely important and subtle point – in our normal physical reality, called the EM state, many of the important qualities of interest are vectors and thus, for a system of multiple parts, there is always an **information entanglement between the parts** unless they are **totally** isolated from each other.
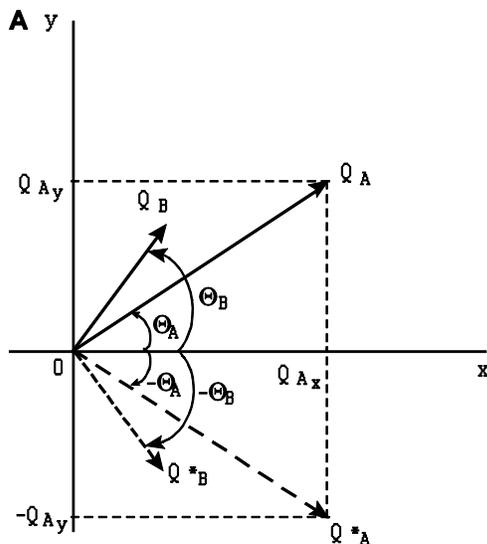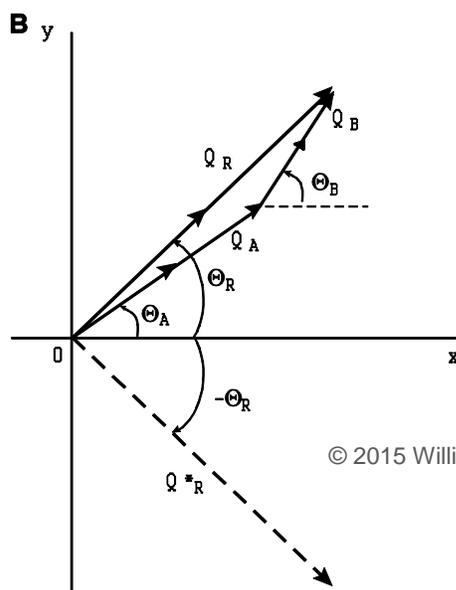

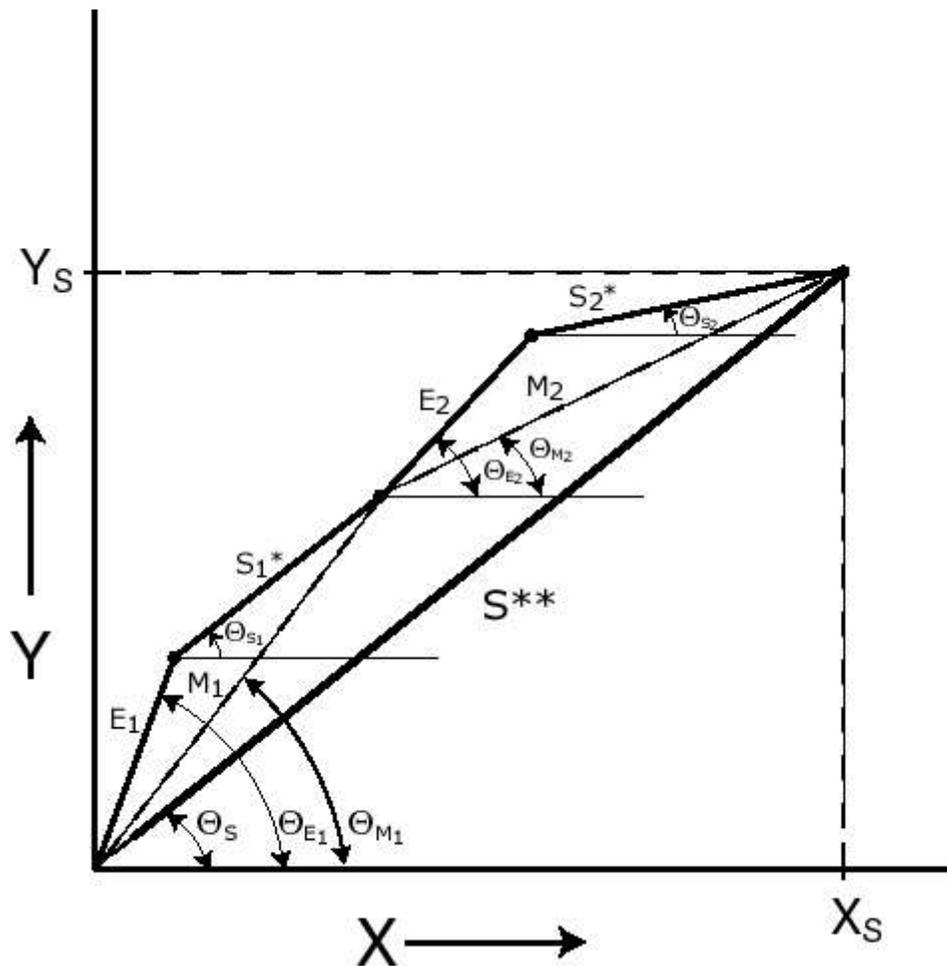Figure 1.   Phasor diagrams for rotating vectors, A. Individual vectors; B. Vector summation.

Figure 2.   Vector summation of two detector systems, M_1 and M_2 to produce S**, the overall system vector.

Figure 1A illustrates two vectors, Q_A and Q_B, their phase angles, θ_A and θ_B, the projected components, Q_{Ax} and Q_{Ay}, plus the complex conjugates, Q^*_A and Q^*_B, (mirror reflection in the x-axis $\rightarrow$ dashed arrows) and Figure 1B illustrates vector addition of Q_A and Q_B to obtain the resultant vector, Q_R, and its complex conjugate (dashed arrow). Figure 2 illustrates the vector situation for two pH-measurement systems where vectors $\underline{E}_1$ and $\underline{S}_1$* add to form $\underline{M}_1$ while vectors $\underline{E}_2$ and $\underline{S}_2$* add to form $\underline{M}_2$ and vectors $\underline{M}_1$ and $\underline{M}_2$ further add to form $\underline{S}$**, the entire system vector.

Although the magnitude of the resultant wave amplitude in Figure 1, $|Q_R|$ is an important quantity, it is the resultant intensity pattern, I_R, that is most important because this is what can be experimentally measured. This is given by the square of Q_R, Q_R^2. Using Figure 1(b) and the Pythagorean Theorem, we have

$$I_R = Q_R^2 = Q_{R_x}^2 + Q_{R_y}^2 = \left[Q_A^2 + Q_B^2\right] + 2\left\{Q_{A_x}Q_{B_x} + Q_{A_y}Q_{B_y}\right\} \qquad (6a)$$

$$= \left[Q_A^2 + Q_B^2\right] + 2Q_A Q_B \cos\left(\theta_A - \theta_B\right) \qquad (6b)$$

and cos means cosine function.

For the Figure 2 example, we have

$$I_S(\underline{k}) = R_S(k)e^{i\theta_S(k)} g R_S(k)e^{-i\theta_S(k)} = X_S^2 + Y_S^2 \qquad (6c)$$

$$= \left(M_1 \cos\theta_{M_1} + M_2 \cos\theta_{M_2}\right)^2 + \left(M_1 \sin\theta_{M_1} + M_2 \sin\theta_{M_2}\right)^2. \qquad (6d)$$

Here, $\underline{k}$ is the R-space vector coordinate, R_S is the system vector amplitude while θ_S is its phase angle. Equation 6d can be expanded further via use of Figure 2. However, perhaps going this far illustrates the complexity of this simple case.

The final step to obtain Q_m is given by

$$Q_m = \int_R I_S(k)dk. \qquad (7)$$

Here, the intensity, $I_S(k)$, must be integrated over all of R-space.

In any particular example of the foregoing, the key steps are:

(1) Define all the key subsystems in the total system that is interacting (often some of these are spatially non-local and even temporally displaced),

(2) Write them all out in vector form (amplitude and phase angle),

(3) Vectorially add them together to form the system vector, $R_S(k)\exp[i\theta_S(k)]$ after having converted all the different measurement units into one common set of units (information change, say),

(4) Obtain the system intensity, $I_S(k)$, by multiplying the system vector by its complex conjugate as in Equation 6c and

(5) Obtain Q_m by performing the integration over R-space via Equation 7.

One of the most interesting results is number (4) above which is illustrated most simply in Equation 6b with the second term where a product of both vector amplitudes appears. In the general case, where N-vectors comprise the total system, a term is present for each vector

pair R_iR_j in the entire system multiplied by a cosine of the phase angle difference, $\theta_i - \theta_j$. This very important term is called the <u>Information Entanglement Term</u> and is always present when the system is in the partially coupled state of physical reality.

As another concrete example, consider the classical case of a standard medical, double-blind study using a particular treatment plus a placebo. The key discriminated elements in this "event" are (1) the doctor or doctors (D), (2) the patient or subjects (s), (3) the particular treatment (T) and (4) the placebo (P). Because the human acupuncture/meridian/chakra system is at the partially coupled state of physical reality, the "event" must be considered to be a "partially coupled state event" in terms of Equation 4. Thus, the $\alpha_{eff}Q_m$ part of Equation 4 (see Equations 6c and 7) involves four coupled vectors of magnitude, R_D, R_s, R_T and R_P and phase angles θ_D, θ_s, θ_T and θ_P. This leads to an information entanglement, I.E., term of the form

$$\text{I.E.} \approx 2\alpha_{eff} \left\{ \begin{array}{l} R_D R_s \cos(\theta_D - \theta_s) + R_D R_T \cos(\theta_D - \theta_T) + R_D R_P \cos(\theta_D - \theta_P) \\ + R_s R_T \cos(\theta_s - \theta_T) + R_s R_P \cos(\theta_s - \theta_P) + R_T R_P \cos(\theta_T - \theta_P) \end{array} \right\} \quad (8)$$

through all the vector pair terms. Here, everything is connected to some degree whose ultimate magnitude increases with the magnitude of α_{eff}. In particular, if the doctors change their collective minds (D) concerning the efficacy of their treatment (T), the I.E. will change in both magnitude and phase angle so $\alpha_{eff}Q_m$ in Equation 4 will change. This type of effect has been reported by Benson[12].

From Equation 8, one can extract a "placebo effect", $\delta(\text{I.E.})_P$, which has the form

$$\delta(I.E.)_P \approx 2\alpha_{eff} R_P \left\{ R_D \cos(\theta_D - \theta_P) + R_s \cos(\theta_s - \theta_P) + R_T \cos(\theta_T - \theta_P) \right\} \quad (9)$$

Thus, one sees from Equations 4 and 9, that a placebo is not an "inert" participant in this event involving the partially coupled state of physical reality. This phenomenon was reported on earlier by one of us[13].

An Application to "Reconnective Healing" Education

We have participated in the monitoring of four Eric Pearl, Reconnective-Healing workshops with our subtle energy detector systems over the past three years, with the fifth event occurring in Los Angeles in late September-early October, 2009. The working

experimental space can be categorized most simply for our pedagogical purpose via Figure 3. Our goal was to continuously
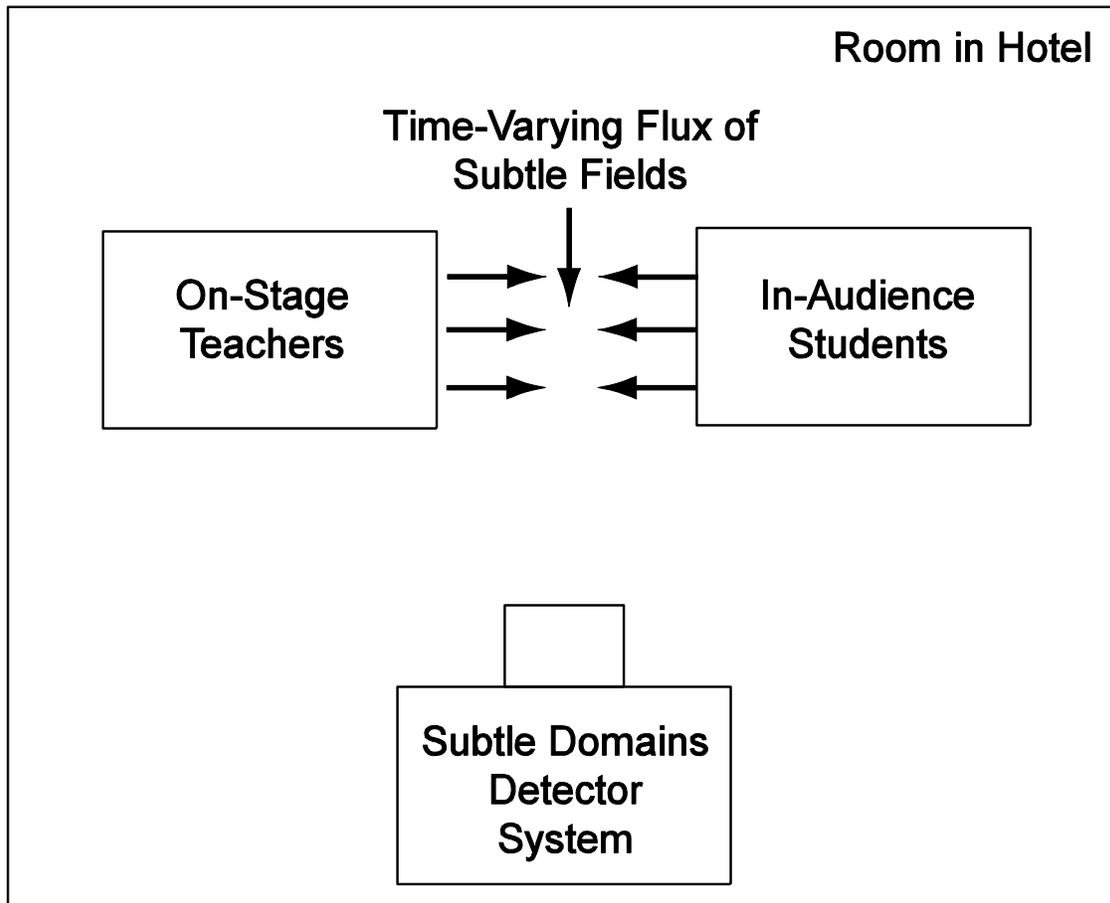

Figure 3. Experimental set-up in a typical Reconnection Workshop.

Measure pH(t), $T_W(t)$ and $T_A(t)$ in the general room environment and, from this experimental data, calculate the state of room conditioning via $\delta G^*_{H+}(t)$ and see how it correlates with the events happening on stage and with the audience.

Figure 4 is data from the opening Friday night July 27, 2007, which we label the "Friday Night Effect". When Dr. Pearl starts doing his lecturing plus energy work. During this period, the <u>magnitude</u> of the <u>excess</u> thermodynamic free energy in the room $|\delta G^*_{H+}|$ increased in a very linear way by ~2.5 milli-electron volts. This change is equivalent to an effective temperature, ΔT_{eff}, change for a normal uncoupled-state room of ~30 ^oC, while the actual room temperature change was only ~4 ^oC. This indicates that the ~2.5 meV change in excess thermodynamic free energy was of a negative entropy change

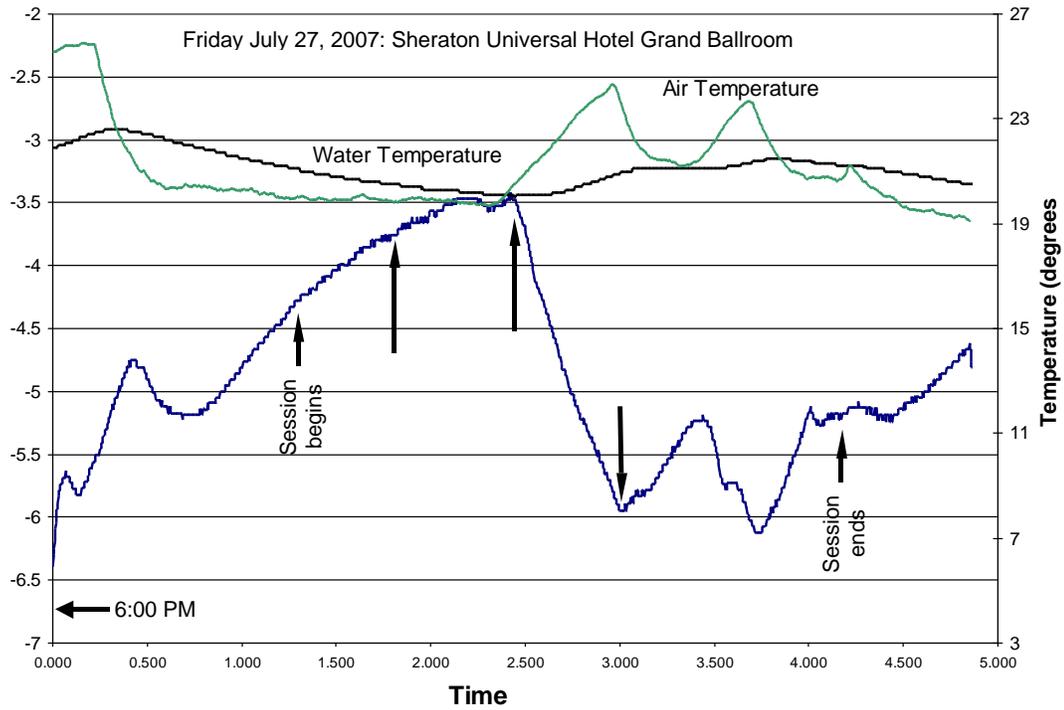type associated with a strong increasing information change process correlated with the event.

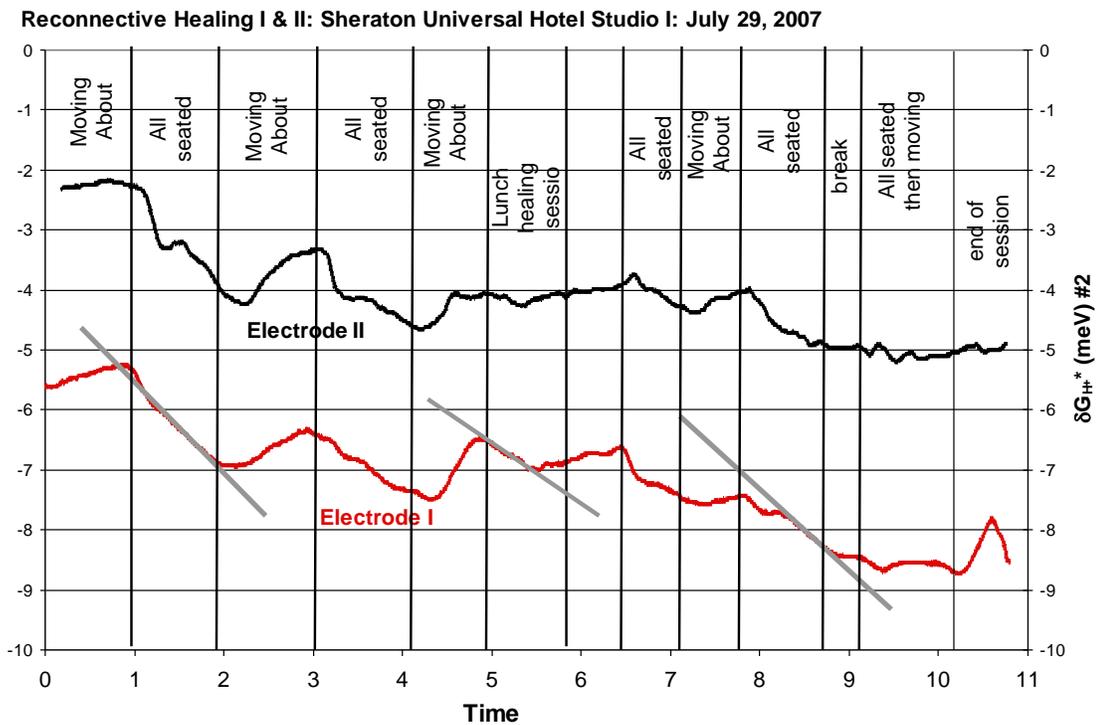Figure 4. $\delta G^*_{H^+}$ for the space vs. time.

Figure 5. $\delta G^*_{H^+}$ for the space vs. time.

Figure 5 shows a two-measurement system use event two days later (recall Figure 2) with other teachers periodically on the stage. If we focus our attention on the electrode I measurement as a function of time, one sees that (a) during speaker on-stage presentations to the seated audience, the <u>magnitude</u> of δG^*_{H+} always seems to <u>increase</u> at ~ a constant slope with time. This signals positive information production and thus thermodynamic entropy annihilation and (b) during audience standing, moving around and talking, the <u>magnitude</u> of δG^*_{H+} always seems to <u>decrease</u>. This signals that net positive entropy production is occurring in the measurement space.

A specific Experiment to Enhance I. E. between Two Sites with D-space Locations ~ 90 Miles Apart

Site-A was located in a specially-constructed shed about 100 yards from the William A. Tiller Foundation laboratory; site-B was located in a SW Phoenix industrial facility about 90 miles distant from site A. Both sites contained identical, continuously running pH, T_W and T_A measurement equipment that was printed out and recalibrated on a weekly cycle. This data was utilized to generate δG^*_{H+}-values at each site for comparison. In this particular experiment, the imprint statement for the intention-host devices to be utilized at sites A and B was the same, one was taken to site A, plugged into a wall socket and switched on while the other was taken to site-B 90 miles away and given the identical treatment.

Figure 6 shows the δG^*_{H+}-correlation at these two sites for weeks 5 to 10 of the experiment. Here we see a remarkably strong correlation, 96%, but of an inverse nature. At site-B, 10 cases of a proprietary product were placed in the measurement space at about week 6.5 and another 10 cases added at about week 8.5; however, no such material was added at site-A.

Figure 7 shows the δG^*_{H+}-correlation for a longer time frame that extended from the beginning of the experiment for 19 weeks. Here, one sees a positive correlation for the first ~4 weeks, but only at the 51.7% level, followed by the Figure 6 negative correlation which was, in turn, followed by 95.5% positive correlation data out to ~ week 19. We do not presently have a clear understanding for the sign reversal of correlation between weeks ~5 to ~10. However, the factory atmosphere would be much more emotionally noisy that the site-A environment.
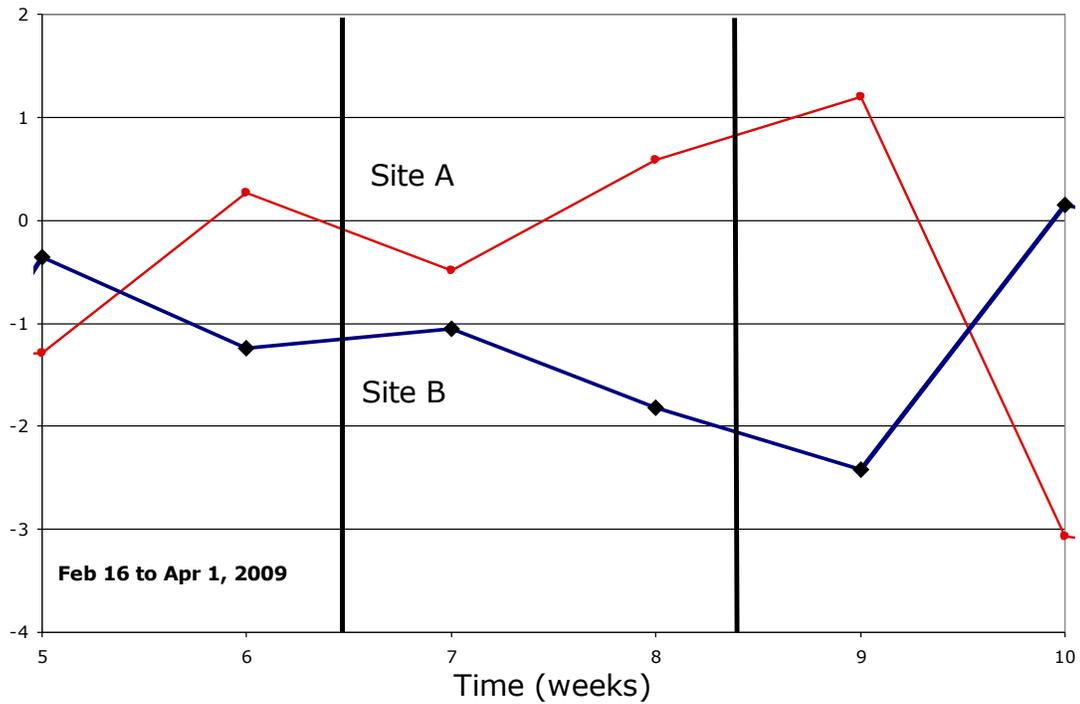
Figure 6.   Weekly average value of δG^*_{H+} vs. time for two sites with identical IIEDs running utilizing the same intention imprint
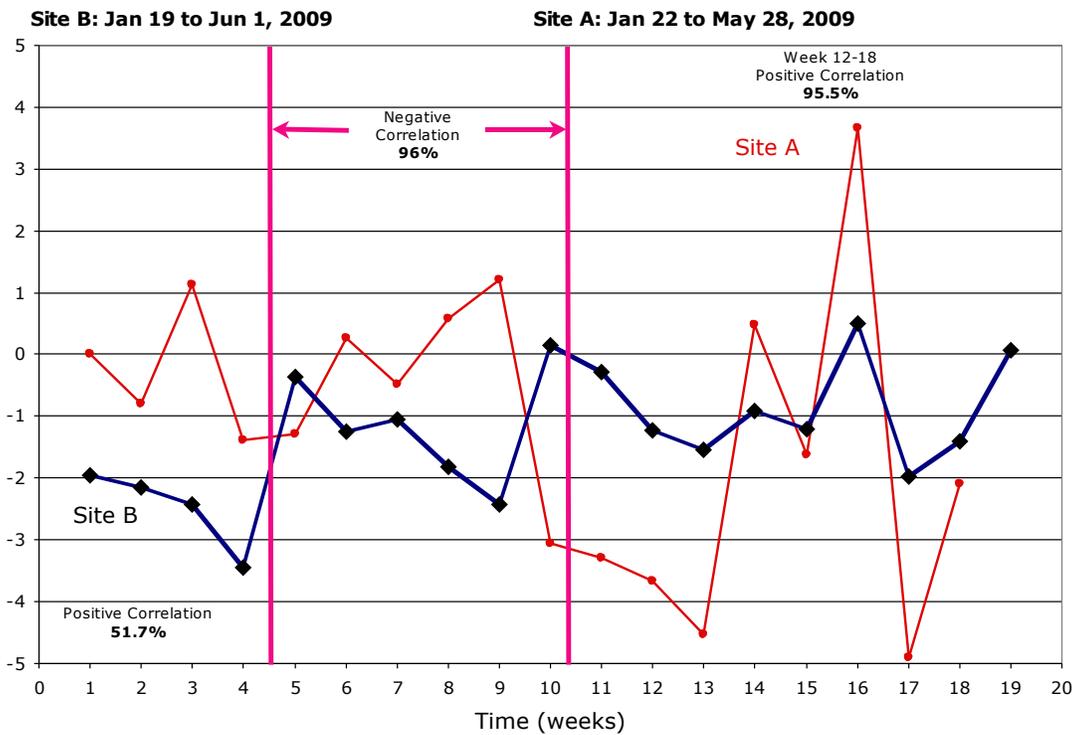

Figure 7.   Weekly average value of δG^*_{H+} vs. time for sites A and B.

In past site-A intention-host device use, δG^*_{H+} would steadily increase to values of ~ 20-30 meV. Some small amount of information entanglement (I.E.) would normally be noticed (at other times) at other external sites where no intention-host device (IHD) was present but that were using our detector system for measurement. However, nothing like Figures 6 and 7 have ever been experimentally experienced before.

If, indeed, we are dealing with a magnetic charge situation in the R-space counterpart of sites A and B, the mathematical expression for the R-space contribution to the thermodynamics is expected to be of the form $\delta G^*_{H+} \approx q_{H+}\phi_{H+}$ where q_{H+} is the net magnetic charge and ϕ_{H+} is the net magnetic potential. From our past experience, δG^*_{H+} for site A has always been positive and large in magnitude whereas, for site B, it has generally been the reverse (but not necessarily large in magnitude). Thus, looking at Figure 6 one might speculate that positive q_{H+} from site-A flows through reciprocal space to site-B to reduce the positive value of ϕ_{H+} for site-A and increase the negative value of ϕ_{H+} for site-B. In such a case, the absolute value, $|\phi_{H+}|$, of ϕ_{H+} does not move far from zero for either site.

Closing Discussion

This is a huge area for future research in coupled state physics. In Chapter 5 of Reference 5, a great deal of experimental data has been presented on local information entanglement between different pH-measurement stations in our Payson laboratory and between an electronic balance station and a closed vs. open window some distance away (regarding R-space geometry of the room in the Payson laboratory). Of course, in the very early days of this work, when we placed an IIED and a UED ~100 meters apart, and both in the electronically-off state, within 3 to 5 days, the information transferred from this IIED to this UED (ME vs. EM information). These are all examples of instrument-instrument information entanglement. In reference 11, White Paper III, the electrodermal diagnostic instrument study represents a good example of human-instrument information entanglement. Many, many examples of this particular type of I.E. exist in the technical literature. Likewise many, many examples of human-human I.E. exist in the literature, but perhaps the most compelling is that provided in reference 14.

As an example to illustrate enhancement of energy/information coupling between humans,[14] consider the situation where two humans (A and B) are wired up for EEG (electroencephalogram) monitoring and placed in separate rooms a short distance apart. Light

stimulation is projected on the closed eyelids of A and this produces a readily distinguishable signature in A's brain waves. Such a signature was also looked for in the brainwaves of B but it was not found. However, when subjects A and B were first asked to sit side-by-side and meditate together for ~10 minutes before the EEG experiment was repeated, this time the special EEG signature was observed to also be present in B's brain waves when A's eyelids were light-stimulated. Here, we propose that an enhanced value of α_{eff} momentarily occurred via the joint meditation process and it was of sufficient magnitude that A-B entanglement could be instrumentally observed.

Figure 8, is presently thought to represent the five essential items that must be considered in any communication event between two or more humans and, in particular, any treatment event between a practitioner and a client. In Figure 8, for the practitioner box, one could also substitute the words spouse, parent, minister, human performer, etc., and correspondingly, for the client box, could substitute the words spouse, child, congregation, audience, etc., respectively. Here, for the client, it must also be realized that they may be strongly R-space connected (via ME radiation fields) to others at distant sites so that the actual experimental system may be larger than it appears on the surface. We are *always* R-space connected to others to some small degree but certain relationships and practices can greatly enhance that coupling.
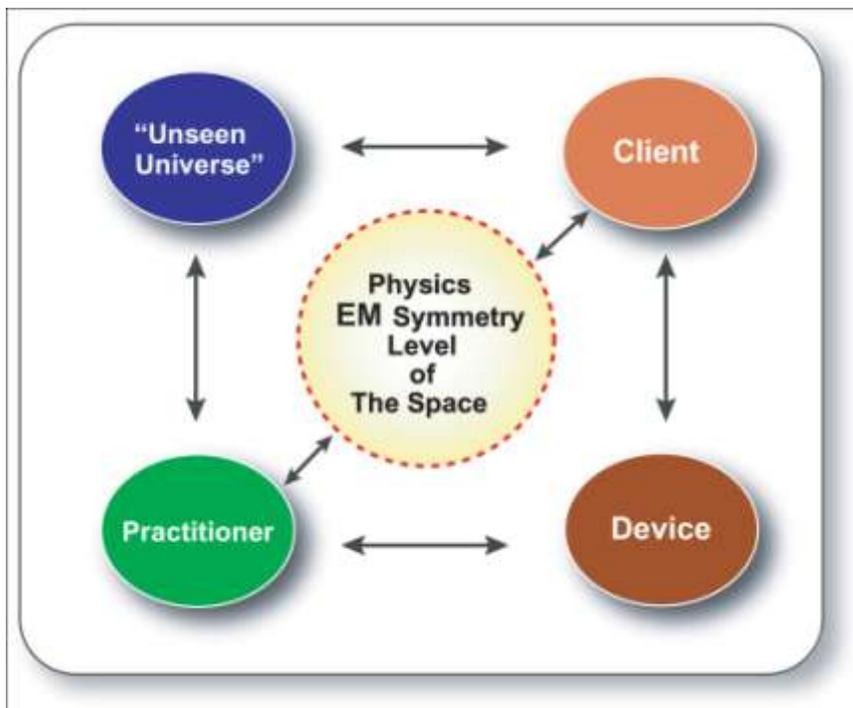

Figure 8. The simplest possible general communication system between practitioner and client in CAM.

As a next to last piece, let us consider the ΔpH=+1 unit replication experiments. Here, we wish to focus first on the spatial information entanglement aspects. How might we come to understand the long-range information entanglement **between** the (P, K and M) IIED laboratory results and the (B_1, B_2, U.K. and Italy) non-IIED laboratory results?

Consider Figure 9. It provides a schematic illustration of D-space and R-space as a construction for discussion purposes. I represent these two, four-dimensional subspaces as parallel, two-dimensional sheets for the simplicity of exposition (as parallel worlds, perhaps) that are initially uncoupled ($\alpha_{eff} \sim 0$). Let us suppose that I set up identical pH-measurement stations at D-space sites A and B, thousands of miles apart and begin to gather background data. Next, I add a ΔpH = +1 unit IIED at the A-station, but not at the B-station. This slowly causes a significant deltron activation to occur in the local environment of A. In turn, this begins to raise the electromagnetic symmetry state of station A at the D-space level.
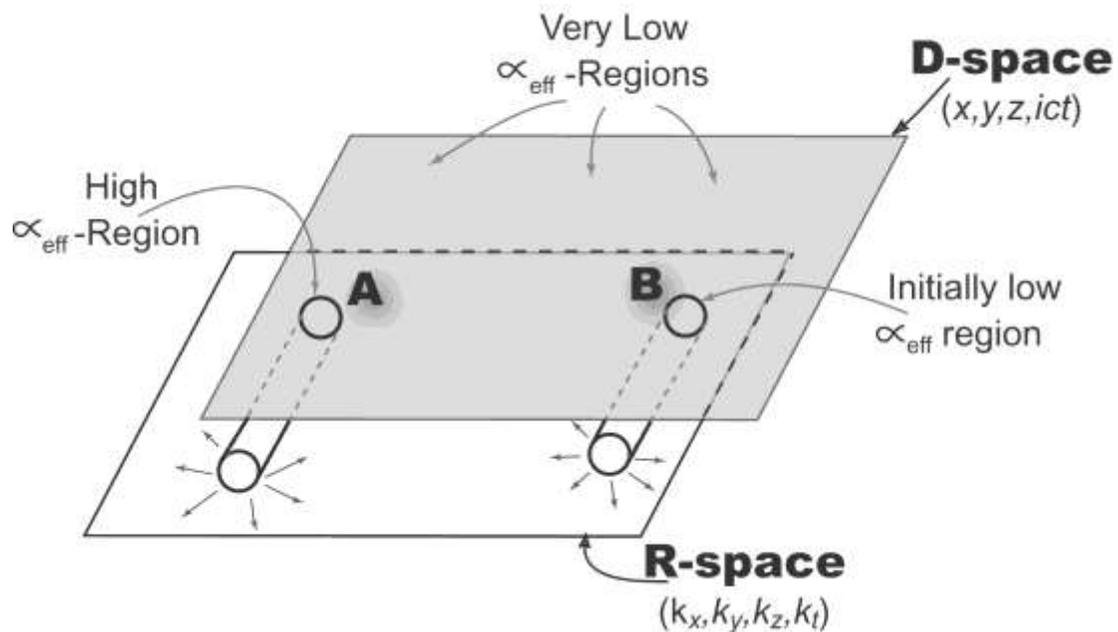

Figure 9.   A schematic illustration of D-space and R-space as a construct.

This means that α_{eff} begins to increase at A and a **thermodynamic driving force** begins to develop for the construction of the equilibrium R-space conjugate amplitude pattern for the D-space measurement equipment and changing pH. This occurs first with the low frequency wave components so the rough outlines of this

equilibrium pattern begins to take shape. Eventually, the high frequency components begin to form so that the fine details of the equilibrium R-space amplitude pattern become highlighted. In this fashion thermodynamic equilibrium between D-space and R-space at station A are thought to develop. However, since R-space is a frequency domain, this magnetic information wave amplitude spectrum is now present **everywhere** as a thermodynamic driving force for change everywhere in D-space even though α_{eff} is only significant at station-A. But, it is only at station-B that identical pH-measurement equipment is present and station-B is the only site, informationally, that is a part of the overall experiment. Thus, the deltron coupling coefficient only begins to develop non-zero values at this D-space site (it requires much more to **materialize** the measurement equipment). Now, the information transfer process occurs at station-B, from the now existing R-space, Station-A equilibrium information wave amplitude pattern, to increase the station-B, α_{eff} value so as to be equivalent with that at Station-A. This is what ultimately converts the measured station-B, pH-value to that of station-A.

Because there are other D-space sites wherein **this process does not occur**, one must conclude that there is an underlying conscious intelligence involved here that selects, to some degree, only those sites that are understood to be part of **our** overall experimental system. This is a very important point that is not, presently, satisfactorily understood.

As a final piece in this information entanglement chain, we would like to address information entanglement in **time**. In mathematically analyzing the spatial profile of air temperature oscillations and the experimental exponential time-dependence of pH-change observed[4,1], we found it absolutely necessary to convert time into a fourth space coordinate, X_4, in the same way Einstein did for his relativity work, in order to mathematically solve the relevant equations. Applying this to our pH-replication procedure, we found that the periodic cyclic water change and electrode recalibration at a remote site could be most simply approximated as D-space spatially periodic impulse events, evenly spaced along the X_4 distance coordinate which information entangle with each other spatially. This concept is illustrated schematically in Figure 10. Here, each of the corresponding R-space impulses decay via the phantom effect processes of Chapter 6 in reference 4 and grow via the information entanglement process from the other impulses of Figure 10. This implies interaction of each impulse with those existing at both larger and smaller X_4-locations. In turn, this means interactions both **forward and backward** in **time**! This is information entanglement in the **time** domain.
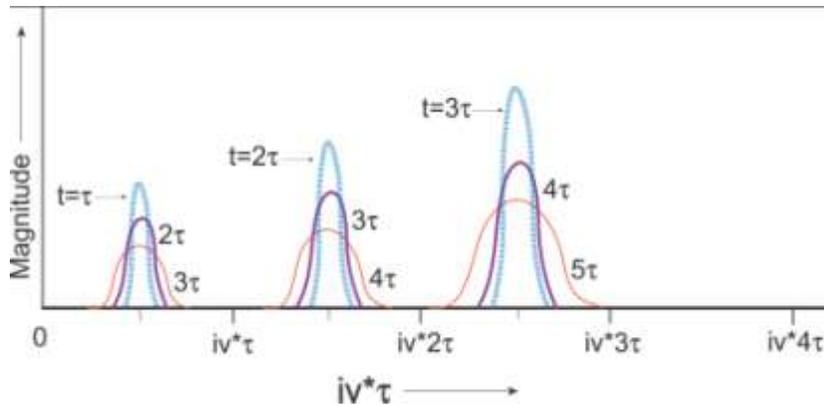
Figure 10. The corresponding R-space impulses decay, via the phantom effect process, and growth via information entanglement from other impulses in the array. This implies interaction both with impulses at larger X_4 locations as well as at smaller X_4 locations which, in turn, means interactions both **forward as well as backwards in time!**

References

1. W. A. Tiller, Psychoenergetic Science: A Second Copernican-Scale Revolution, (Pavior Publishing, Walnut Creek, CA, USA, 2007).

2. W. A. Tiller and W. E. Dibble., Jr., White Paper I, A Brief Introduction to Intention-Host Device Research, www.tiller.org

3. L. Brillouin, Science and Information Theory, 2nd Ed, (Academic Press, New York, N.Y., 1962, Chapter 12).

4. W. A. Tiller, W. E. Dibble, Jr., and M. J. Kohane, Conscious Acts of Creation: The Emergence of a New Physics (Pavior Publishing, Walnut Creek, California, 2001).

5. W. A. Tiller, W. E. Dibble, Jr. and J. G. Fandel, Some Science Adventures with Real Magic, (Pavior Publishing, Walnut Creek, California, 2005).

6. M. A. Nielsen, "Rules for a complex quantum world?, Scientific American, 287 (5) (2002) 67.).

7. A. D. Aczel, Entanglement (A Plume Book, Penguin Group, London, 2003).

8. S. Ghosh, Nature 425 (2003) 48.

9.   M. C. Arnesen, S. Bose and V. Vedral, "Thermal Entanglement in 1D Heisenberg Model", Phys. Rev. Lett. <u>87</u>, 017901 (2001).

10.   B. Reznik, "Entanglement from the Vacuum", Foundations of Physics, <u>33</u> (1) 167-176, January 2003.

11.   W. A. Tiller, White Paper III, <u>Why CAM and Orthodox Medicine Have Some Very Different Science Foundations</u>, www.tiller.org

12.   H. Benson and M. Stark, <u>Timeless Healing: The Power and Biology of Belief</u> (Scribner, New York, N.Y., 1996).

13.   W. A. Tiller, "Human Psychophysiology, Macroscopic Information Entanglement and the Placebo Effect", JACM <u>12</u> (10), 2006, pp1015-1027.

14.   J. Grindberg-Zylerbaum, M. Delafor, L. Attie and A. Goswami, Physics Essays <u>7</u> (1994) 422.